Journal of Structural Geology 30 (2008) 993–1004

Contents lists available at ScienceDirect

Journal of Structural Geology

journal homepage: www.elsevier.com/locate/jsg

Predictive permeability model of extensional faults in crystalline and metamorphic rocks; verification by pre-grouting in two sub-sea tunnels, Norway

Guri Venvik Ganerød [a,b,*], Alvar Braathen [b,c], Bjørn Willemoes-Wissing [a]

[a] Geological Survey of Norway, 7491 Trondheim, Norway
[b] Department of Earth Science, University of Bergen, 5007 Bergen, Norway
[c] Department of Geology, University Centre in Svalbard, 9171 Longyearbyen, Norway

ARTICLE INFO

Article history:
Received 5 October 2007
Received in revised form 1 April 2008
Accepted 1 April 2008
Available online 10 April 2008

Keywords:
Permeability
Extensional faults
Fault zones
Fracture distribution
Cement injection
Sub-sea tunnels

ABSTRACT

This paper link quantitative fault zone descriptions, qualitative fracture and fault rock properties, and engineering data in the study of the permeability structure of fault zones. Datasets include scan-lines, drill cores and cement pre-grouting from two sub-sea tunnels in gneissic and granitic rocks, from which systematic pre-grouting volumes can be used to analyse the in-site relative permeability both in host rocks and fault zones. Major extensional faults intersected by the tunnels reveal common fault rocks surrounding intensively fractured rock lenses in the core. Fracture frequencies in these lenses can reach 100 fractures/metre (f/m). In the bounding damage zones, networks of fracture sets make up an inner zone of fairly high frequency (20–30 f/m) of fault-parallel, long fractures connected by shorter fractures. An outer zone has lower frequencies (<20 f/m) and more diverse fracture orientations and lengths. There is a general increase in fracture frequency from the background level of the protolith towards the fault core.

Tunnel-scale injection of cement reveals patterns that can be ascribed to the impact of faulting; there is an increase in cement injection in fault zones compared to areas with background fracturing away from faults. In detail, there is an innate division of the rock volume into sub-zones characterized by distinct structural style and permeability, with a background level and three fault related sub-zones (fault core, inner damage zone, and outer damage zone). Injection data shows that the background sub-zone commonly can be injected with less than 0.05 m^3 cement per metre tunnel (commonly not injected), whereas the fault core has permeability characteristics nearly as low as the outer damage zone, represented by 0.1–0.2 m^3 cement per metre tunnel, with occasional peaks towards 0.5 m^3. The maximum of cement injection lies in the inner damage zone, marginal to the fault core, with 0.3–0.7 m^3 cement per metre tunnel, locally exceeding 1 m^3. This gives a relative relationship for cement injection of approximately 1:2:1 between fault core, inner damage zone, and outer damage zone of extensional fault zones in crystalline and metamorphic rocks.

1. Introduction

Faults represent a challenge in all type of engineering projects, especially in tunnels and quarries, because of increased fracture density, weak rocks, poor rock stability, and enhanced fluid flow (e.g., Hoek and Bray, 1981; Hoek, 2000; Nilsen and Palmstrøm, 2000; Blindheim and Øvstedal, 2002). In sedimentary basins, faults are often analysed due to sealing capacity of gas, oil, and groundwater (e.g., Manzocchi et al., 2008). Faults also represent a major hazard to mankind, in that they locate repeated earthquakes that can be devastating, for example seen along the San Andreas Fault (Chester et al., 1993; Chester and Chester, 1998; Evans and Chester, 1995). Earthquakes magnitude and reoccurrence are linked to fault core mechanical strength (Chester et al., 1993). These subjects have promoted significant attention around faults, with focuses spanning from fault arrays and displacement fields (e.g., Walsh et al., 2003a,b), to intrinsic fault geometry and fault architecture (e.g., Chester et al., 1993; Caine et al., 1996; Braathen et al., 2004; Collettini and Holdsworth, 2004), and into the realm of frictional behaviour, linked to mechanical and chemical processes (Sibson, 1986, 2000; Stewart et al., 1999; Braathen et al., 2004). Major faults truncate a significant part of the crust, and will reveal

* Corresponding author. Geological Survey of Norway, Underground Construction, Leiv Erikssons vei 39, 7491 Trondheim, Norway. Tel.: +47 7390 4313; fax: +47 7392 1620.
E-mail address: guri.venvik.ganerod@ngu.no (G.V. Ganerød).

0191-8141/$ – see front matter © 2008 Elsevier Ltd. All rights reserved.
doi:10.1016/j.jsg.2008.04.001

different fault products (mylonites, cataclasites, breccias) related to depth, temperature, strain rate, and internal processes, as the fault is unroofed (Sibson, 1986). Fluids play an important role in weakening and generating of faults in general (Chester et al., 1993; Collettini and Holdsworth, 2004; Faulkner and Rutter, 2001, Faulkner et al., 2003; Seront et al., 1998; Sibson, 1986, 2000; Wibberley and Shimamoto, 2003) and, from an applied point of view; fault zones tend to host ground water.

In this work, we combine fault rock descriptions related to polyphase activity during faulting and unroofing, with damage zone fracture properties, and with engineering data. The uniqueness in the work relates to the connection between structural observations that can be linked with pre-grouting cement volumes in two sub-sea tunnels. This opens for in situ considerations of the permeability structure of fault zones.

2. Fault models and permeability

The established terminology on fault zone architecture in metamorphic and crystalline rocks (Caine et al., 1996; Seront et al., 1998) is the fault core, damage zone and protolith. Fault models outline a core that has seen the bulk of displacement, and is therefore hosting fault rocks. Outside this, deformation is accommodated mainly by fractures of the damage zone. The boundary between core and damage zone is typically sharp, and defined by slip surfaces (shear fractures), whereas the transition between damage zone and protolith is marked by a decrease in fracture intensity, to a regional background frequency level. These models predict a zoned permeability field in fault zones in crystalline rocks (Caine et al., 1996; Evans et al., 1997; Wibberley and Shimamoto, 2003), where typically a low permeability fault core is surrounded by a more permeable damage zone toward pristine, lower or impermeable host rocks. Protolith rocks have neglectable primary porosity and permeability unless damaged by brittle deformation (Norton and Knapp, 1977; Morrow and Byerlee, 1988, 1992; Morrow and Lockner, 1997).

In the damage zone, the fracture intensity shows a significant increase in frequency from the background level towards the fault core (Caine et al., 1996; Braathen et al., 1998). Not only the frequency but also the length of fractures is of interest, since a key conclusion from simulation of flow in fracture systems is that long fractures will conduct more water than short fractures, due to higher connectivity (Odling, 1997). Detailed analyses of damage zones reveal sub-zones characterized by distinct fracture sets and populations, as outlined in Braathen et al. (1998). They describe a core of fault rocks surrounding lenses of host rock with a dense network (20–100 f/m) of short fractures. The damage zone has an inner part, 5–50 m wide, dominated by fault-parallel, moderate frequency long fractures, which are connected by shorter fractures. In total, this gives an overall good connectivity. The outer part of the damage zone shows decreasing frequency of fractures that varies in length and orientation, demarcating the transition from damage zone to background fracture level.

Permeability models of faults combine numerical simulations with laboratory permeability measurements (Morrow and Byerlee, 1988, 1992; Morrow and Lockner, 1997; Seront et al., 1998; Faulkner and Rutter, 2001). The latter is almost in all cases based on fairly small samples or rock analogues due to the limitations in instrumentation. For example, Faulkner and Rutter (2001) show that phyllosilicate-bearing fault gouge has permeability in the range of $\sim 10^{-18}$ to $\sim 10^{-21}$ m^2 based on oriented drill core samples. In other words, their gouge has sealing capacity, and can act as a barrier or baffle to fluid flow in fault zones. In another study of samples from drill cores, Morrow and Byerlee (1988, 1992) show that the permeability of intact crystalline host rock range from 10^{-18} to 10^{-22} m^2 at effective pressures equalling depths from 270 to 3500 m. The latter study confirms that the permeability of rocks and fractures is reduced with depth, i.e. with increasing effective pressure (Morrow and Byerlee, 1988, 1992; Morrow and Lockner, 1997). In accordance with the studies presented above, permeability studies aimed on faults at shallow depth show that the lowest permeability is found in the fault core, as addressed by for example Seront et al. (1998). Their field and laboratory results suggest that the damage zone conduct most fluid due to its higher values of permeability, which are several orders of magnitude higher than the protolith and the core. These results are undermined by Faulkner and Rutter (2001), who question the value of laboratory test results in which the natural fault rocks are without intact in situ fabrics. Anyhow, Evans et al. (1997) conclude that there is a permeability contrast between fault core and damage zone in the order of magnitude of 10–10^4, with a maximum contrast of 10^6. Further, they argue that the permeability field is anisotropic, in an order of 10^4, with the highest permeability parallel to the fault.

Another approach to permeability assessments of faults goes through in situ analysis of tunnels, by continuous surveying of water leakage and countermeasures to water leakage and instability by cement injection. In the presented two case studies of sub-sea tunnels that transect regional scale extensional faults in metamorphic and crystalline rocks, permeability is addressed through tunnel-scale injection (pre-grouting) of cement. Presented data show regular permeability contrasts within faults, consistent with observable structural zoning. The cases presented are the Frøya and Oslofjord tunnels in central and south-eastern Norway, respectively (Fig. 1).

3. Methods and datasets

Presented datasets include scan-lines, drill cores and pre-grouting cement volumes. The main dataset on structures is from drill cores, which implies that the fault zones and their subordinate parts are classified from this data set. Note that the fracture frequency in drill cores is regarded as higher than insitu fracture frequency due to the applied stress during drilling. When tunnel surveying and engineering logs have allowed identification of footwall and hanging-wall sides of faults, this is added to the description. The drill cores were collected in the tunnel during construction, commonly sampling rocks 15–25 m ahead of the tunnel face at the time of excavating. They have been mapped with respect to lithology and logged continuously for fracture frequency with the unit fracture per metre (f/m). Measuring true aperture or orientation of fractures in the drill cores was not viable due to mobility of the cores during drilling and within the storage boxes, and the drill cores are not oriented. Locally, the coverage of drill cores is variable and especially along stretches of un-fractured host rock, drill cores have not been collected and/or stored. In addition, where the rock has poor quality, as in fault cores, core loss is common. To quantify the fault zones, and for plotting purposes, class values of fracture frequencies were pre-set for occurrence of (non-cohesive) fault rocks, representing breccia (50 f/m) or gouge (70 f/m). All frequencies below these thresholds are measured fracture frequency. Description of fault rocks is reached through the descriptions and classifications presented in Braathen et al. (2004).

Tunnel data include measured fracture frequency in scan-lines along the foot of the tunnel wall, and was collected during tunnel excavation for the Oslofjord tunnel only. Data was obtained in intervals ranging from 5 to 15 m. For simplicity, the tunnel mapping was performed with preset values for fault rocks (60 f/m) and fault rock with lenses hosting a dense fracture network (40 f/m). Values below this level represent actual fracture frequency. In construction of road tunnels, production safety regulations combined with immediate installation of concrete cover on faults, due to stability and

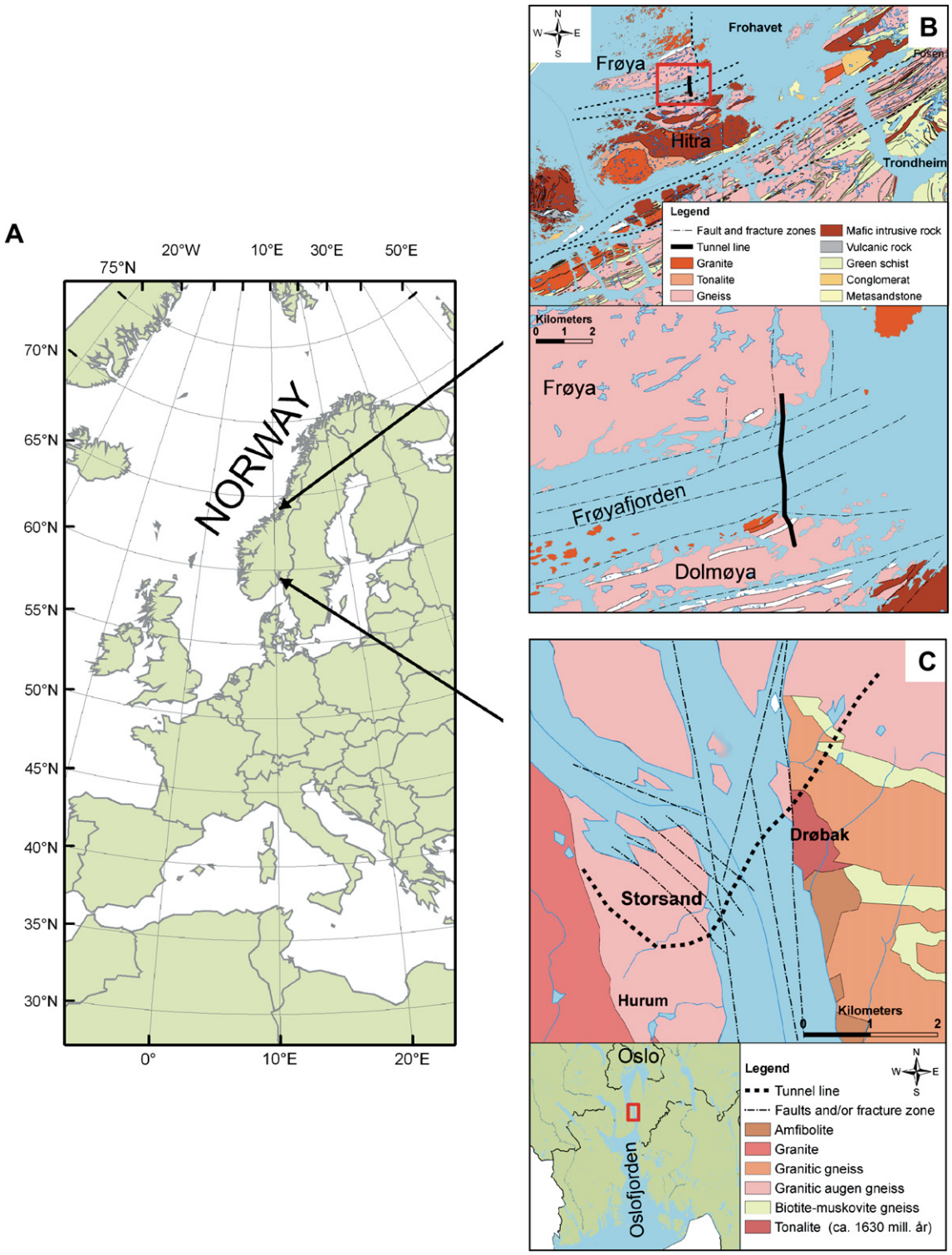

Fig. 1. (A) Location of the two sub-sea tunnels studied; the Frøya tunnel in central Norway and the Oslofjord tunnel in southern Norway. (B) The Frøya tunnel of central Norway connects the islands Frøya and Dolmøya underneath the Frøyfjorden strait. The region is affected by the Møre- Trøndelag Fault Complex (MTFC) that runs sub-parallel to the coast into the offshore domain (Grønlie et al., 1991; Sættem and Mørk, 1996; Bøe et al., 2005; Redfield et al., 2005). The bedrock geology of the Frøya and Hitra islands is dominated by granites and gneisses (Nordgulen, 1995). (C) The Oslofjord road-tunnel stretches from Storsand (Vestfold County) in the west to Drøbak (Akershus County) in the east, crossing the Drøbak strait of the Oslofjord. The Oslofjord sub-sea tunnel is 7.2 km long, where 2.4 km is under the fjord. Three major segments of the Oslofjorden Fault Complex (OF) are located in the strait, with the most prominent segment to the east (Palmstrøm et al., 2003). The OF separates mainly Cambro-Silurian and Permian sedimentary and volcanic rocks to the west from Precambrian basement gneisses to the east (Lutro and Nordgulen, 2004), however, the tunnel is entirely in gneisses and granites.

safety measures, made it impossible to carry out complete tunnel mapping in the Oslofjord tunnel.

Pre-grouting, i.e. injection of cement through drill holes ahead of the tunnel head during excavation, was performed according to predefined pressure thresholds. Pumping/injection pressure was initially set to 45 bar for both tunnels, with a maximum reaching 60 bar. Occasionally, pressure was up to 70–80 bar (Lien et al., 2000; Blindheim and Skeide, 2002). If the rock was still permeable

at this pressure, the cement was changed to a more viscous cement type. Therefore, the recorded volumes of cement may be seen as minimum values. During the tunnel constructions, 3–4 types of cement ranging from fibrous to armoured are applied, with densities varying from 2800 to 3200 kg/m^3, with an average of 3000 kg/m^3, and with different viscosity properties. The heavier, armoured cement type is commonly reserved for heavily fractured and loose rock, commonly found around the fault core, and is used mainly for stability reasons. Initial injection was performed in 23 holes of 20 m length drilled ahead of the blast hole. If injection did not reach the preset pressure threshold, this was increased to 28 holes of 23 m length, with maximum length of 30 m, to reduce the injection spacing (Lien et al., 2000; Blindheim and Skeide, 2002).

4. The Frøya tunnel

The Frøya tunnel, which was started in year 1999 and finished in 2000, runs N–S underneath the Frøyfjorden strait from the Frøya Island southwards to the Dolmøya Island (Fig. 1B). The tunnel has a total length of 5.3 km, of which 3.6 km is sub-sea. The lowest point is 162 m below sea level. For published work on the Frøya tunnel, see Bøe et al. (2005), Lien et al. (2000), Lillevik et al. (1998), and Sættem and Mørk (1996).

The Frøya Island (Fig. 1B) is made up of granites and gneisses related to the Scandinavian Caledonides of Mid Silurian to Mid Devonian age (Gee et al., 1985). In more detail, the bedrock geology of the Hitra, Dolmøya and Frøya islands is dominated by the Smøla-Hitra batholith (Nordgulen et al., 1995). The batholith intrudes Precambrian supracrustal rock, the latter with medium- to high-grade metamorphic fabric (Askvik and Rokoengen, 1985). On Frøya Island, the bedrock alters from tonalite in the west, to granite and migmatite in the north, and banded migmatitic gneiss in the central and southern parts (Askvik and Rokoengen, 1985). Underneath the Frøyfjorden strait, common rocks are tonalite to granite, which locally host lenses of metasedimentary rock such as marble. Devonian molasse basins and Jurassic extensional basins are found south, east and west of the Frøya Island and are all associated with fault activity along the Møre- Trøndelag Fault Complex (MTFC).

The key structure of the region is the MTFC, which is a crustal-scale, NE–SW to ENE–WSW trending fault complex. This fault complex has several parallel fault strands, running along the coast of central Norway (e.g., Gabrielsen et al., 2002). One strand, the Frøyfjorden fault, is located between the islands of Frøya and Hitra. Nearby in the offshore, this fault defines the south-eastern boundary of a Jurassic basin, the Frohavet basin (Bøe et al., 2005). The Frøyfjorden fault array consists of at least four large, ENE–WSW trending, sub-parallel segments (Fig. 1B; Sættem and Mørk, 1996; Bøe et al., 2005), of which several were cut by the sub-sea tunnel. Other structures of the area include N–S and NE–SW lineaments, which are also abundant in the Frøyfjorden strait (Braathen, 1996; Sættem and Mørk, 1996; Bøe et al., 2005).

Repeated fault activity within the Frøyfjorden fault array is documented by movements during the Devonian and Jurassic (Grønlie et al., 1991; Sættem and Mørk, 1996; Bøe et al., 2005; Redfield et al., 2005). Further, uplift of the mid-Norwegian shelf during the Cretaceous and Tertiary caused reactivation of segments within the MTFC (Redfield et al., 2005), which may tie to non-consolidated fault rocks recorded in the Frøyfjorden fault array (Sættem and Mørk, 1996; Bøe et al., 2005). This chronology is confirmed in outcrops of faults on the Frøya Island and elsewhere in the region, which reveals several types of fault rocks, ranging from semi-ductile mylonites to cataclasites and non-cohesive breccias and gouge (Eliassen, 2003; Grønlie et al., 1991; Osmundsen et al., 2006).

The tunnel surveying established a total of ten synthetic (N-dipping, similar to the Frøyfjorden fault) and five antithetic (S-dipping) fault and/or fracture zones, where the largest ones run approximately ENE–WSW, sub-parallel to the Frøyfjorden strait (Figs. 1B and 2). In general, excavated fault zones are approximately 100 m wide. They host one or more, decimetre to metre wide fault core of both cohesive and non-cohesive fault rocks, which is surrounded by fracture sets of the damage zone.

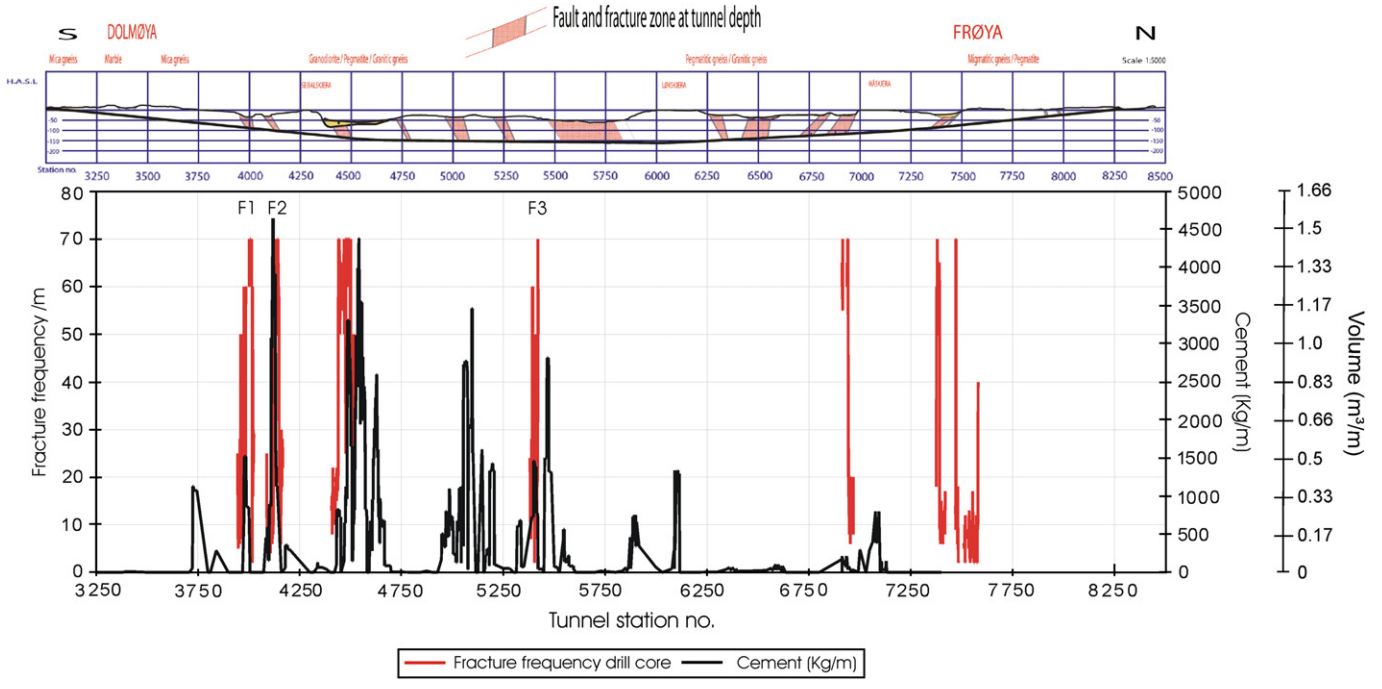

Fig. 2. Cross-section showing faults and/or fracture zones (red) encountered in the Frøya tunnel. The plot presents injected cement volumes per metre and fracture distribution recorded by drill core logging along the tunnel.

Drill cores from the tunnel reveals foliation in the protolith bedrock, however, the fabric is not pervasive. The boundary between protolith and fault cores are commonly sharp (Fig. 3). The latter is made up of either: (i) basically impermeable protocataclasites to cataclasites hosting protolith fragments in the range from 0.2 to 0.5 cm to several centimetre; or (ii) red (from hematite) carbonate cemented breccia with fragments of the protolith and cataclasites in the size of millimetre to centimetre (Bøe et al., 2005). The latter breccia, which is basically without preserved porosity, dominates (Fig. 3A). These fault rocks are rejuvenated in two types of late porous breccias; (iii) breccia with reworked cataclasite and with fragments of carbonate cemented breccia, commonly having a fine-grained green coloured matrix (Fig. 3C); and (iv) breccia hosting fragments of protolith (Fig. 3B), frequently occurring in the contact between the protolith and cataclasites. Breccias range from grain supported protobreccia with up to 5 cm fragments, to matrix supported ultrabreccia with fragments between 0.2 and 0.5 cm. Encountered gouge, commonly with a red or green colour, is very fine grained and almost entirely made up of matrix (Fig. 3C). The gouge likely has permeability values similar to that reported by Faulkner and Rutter (2001), hence it is nearly impermeable. When gouge is found in association with cataclasite, the gouge layers of reworked cataclasite are narrow. Contrary, when related to breccias, the gouge layers can be from 0.5 to 2 m wide. In total, the drill cores show that the amount of non-cohesive fault rocks is superior to that of cohesive fault rocks.

In the drill cores of the Frøya tunnel, the background fracturing is relatively high, commonly around 5–7 f/m (Fig. 4). Increased fracture frequency is encountered in the approximately 100 m wide fault zones, showing increasing fracture frequency towards the major fault cores. The outer damage zone has a fracture frequency below 20 f/m whereas the inner damage zone ranges between 20 and 30 f/m. The core of the fault has a width of 2–30 m, as shown by the predefined fracture frequencies for fault rocks (between 50 and 70 f/m), seen in Fig. 4.

Cement injection in the Frøya tunnel was performed as pre-grouting through the entire tunnel and was most extensive on the southern side of the fjord (Fig. 2), near the main Frøyfjorden fault. The background volume of cement injection is less than 100 kg/m (0.03 m^3 per metre tunnel) while the highest volume related to a fault is 4651 kg/m (1.55 m^3/m, Figs. 2 and 4). In total, 1043 tons (347.66 m^3) cement was injected into the sub-sea tunnel, of which the majority is associated with faults.

In the tunnel, the mentioned injection peak of 1.55 m^3 per metre tunnel relates to an N-dipping fault with 30 m wide core (stations 4120–4150, Fig. 4). The latter consists of intensely fractured rock and thin gouge layers, of which the thickest gouge membrane is 0.5 m wide. This fault caused significant water leakage and was handled by extensive cement injection, with a total volume of 98 tons (32.66 m^3, Lillevik et al., 1998). Most of this injection volume was located in the footwall part of the core and in the nearby, bounding damage zone, as shown in Fig. 4. This pattern of core-marginal injection peaks is similar to that encountered for many faults in the tunnel (see Section 6).

5. The Oslofjord tunnel

The Oslofjord road-tunnel starts at Storsand (Vestfold County) in the west and surfaces near Drøbak (Akershus County) to the east

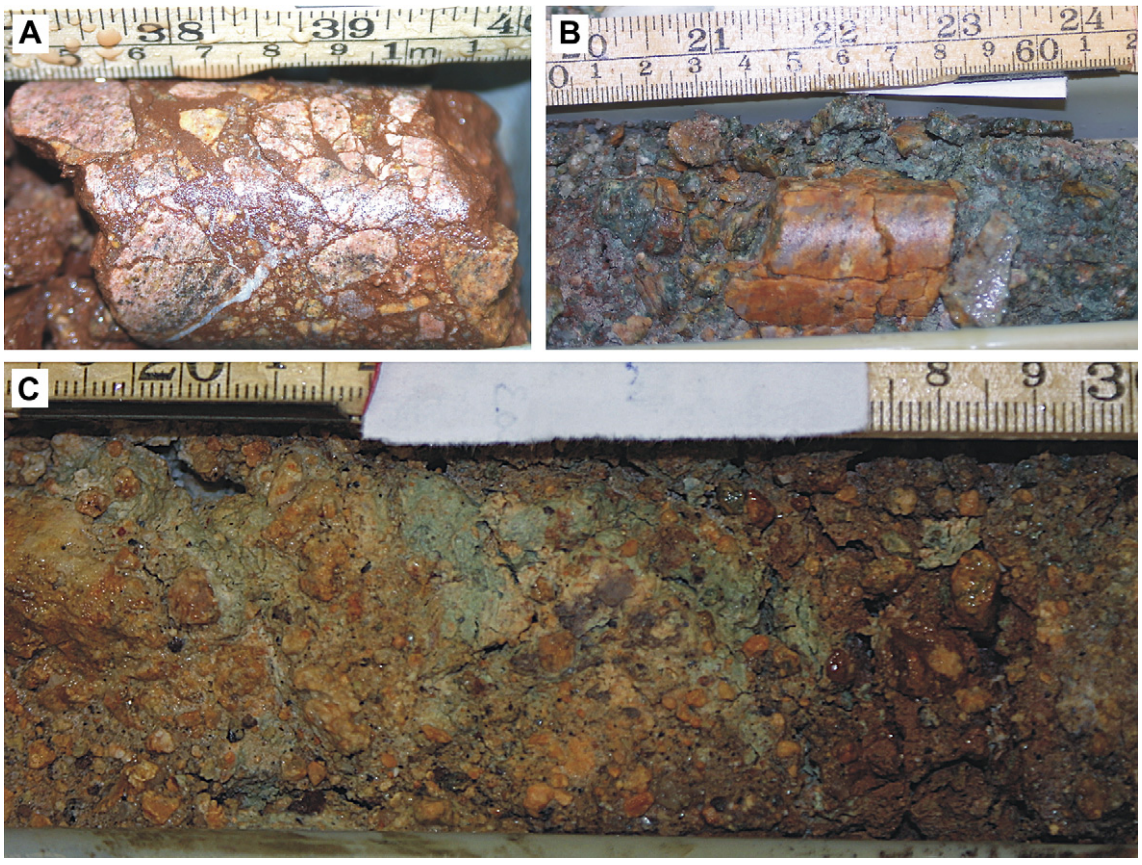

Fig. 3. Example of fault rocks encountered in the Frøya tunnel, where a range of fault rocks commonly occur in the fault cores. (A) Red (hematitie), carbonate cemented breccia hosting protolith fragments in the range of 0.2–3 cm. (B) Porous protobreccia with fragments of protolith in the size-range of 0.5–5 cm, in contact with protolith of granite (right). In the core box, the protolith can be seen to alter into a protobreccia (as in B) that evolves into a breccia and further into (C) an ultrabreccia and gouge.

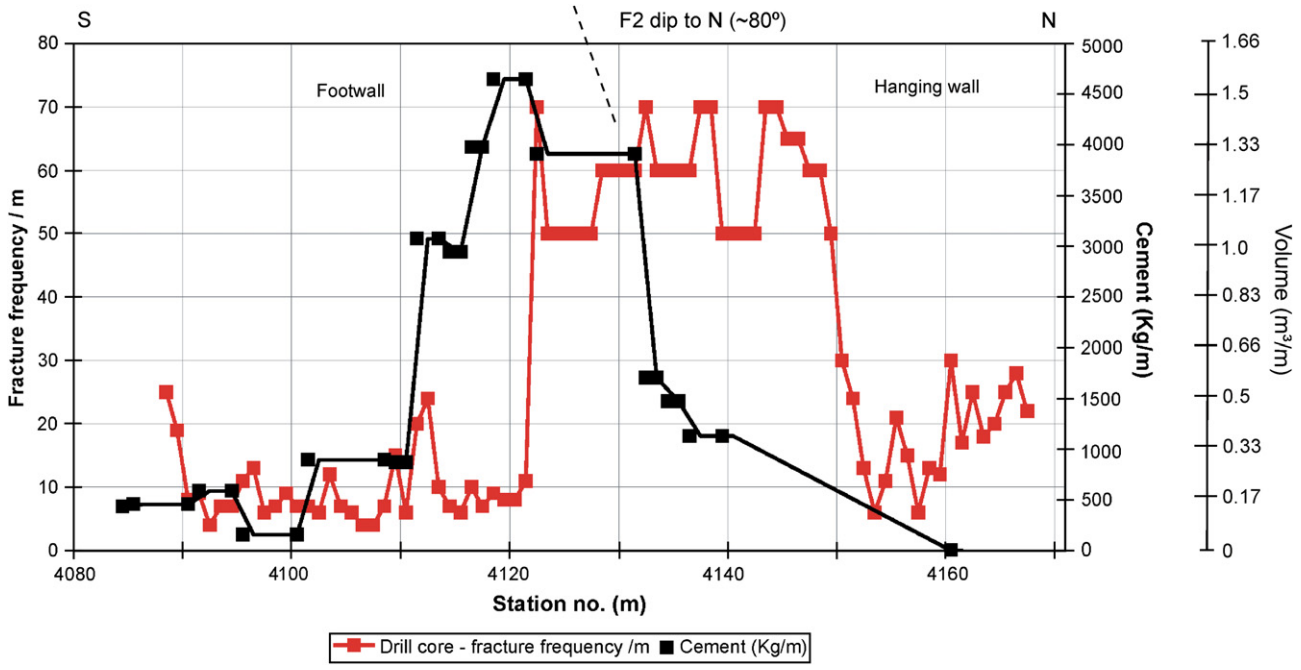

Fig. 4. Fracture distribution from drill cores logs correlated with volume of injected cement for a tunnel section, station no. 4080–4170, in the Frøya tunnel. This zone had the highest water leakage and required the most pre-grouting in the tunnel. The peak of cement injected (st. no. 4120) lies towards and in the inner damage zone on the footwall side of the fault zone, in the plot to the left of the less permeable fault core (st. no. 4124–4150).

(Fig. 1C). The tunnel has a total length of 7.2 km of which approximately 2.4 km are below the Drøbak strait of the Oslofjord. Tunnel construction started in spring 1997 and was completed during the summer of 2000. For published work on the Oslofjord tunnel, see Blindheim and Øvstedal (2002), Blindheim and Skeide (2002), and Palmstrøm et al. (2003).

The geology of the Oslofjord region is divided into a western province of Cambro-Silurian to Permian sedimentary and volcanic rock successions, and an eastern Precambrian province of plutonic rocks and gneisses (Fig. 1C; Heeremans et al., 1996; Lutro and Nordgulen, 2004). Drill cores from the Oslofjord tunnel show that the protolith bedrock is mainly granitic gneiss, rich in quartz and feldspar, and characterized by augen structure and bands of mafic composition. The N–S to NE–SW trending Oslofjord Fault Complex (OF) separates the two regions. The OF is a major block-bounding structure that can be traced from the Oslo City and nearly 100 km southwards into the Skagerrak Sea, consistently making up the eastern boundary of the Permian Oslo Graben (Swensson, 1990; Heeremans et al., 1996; Lutro and Nordgulen, 2004). The OF has a down-to-the-west throw of about 2–3 km near Oslo that increases to the south. Good exposures of a fault segment, the Nesodden fault, reveal both cohesive and non-cohesive fault rocks

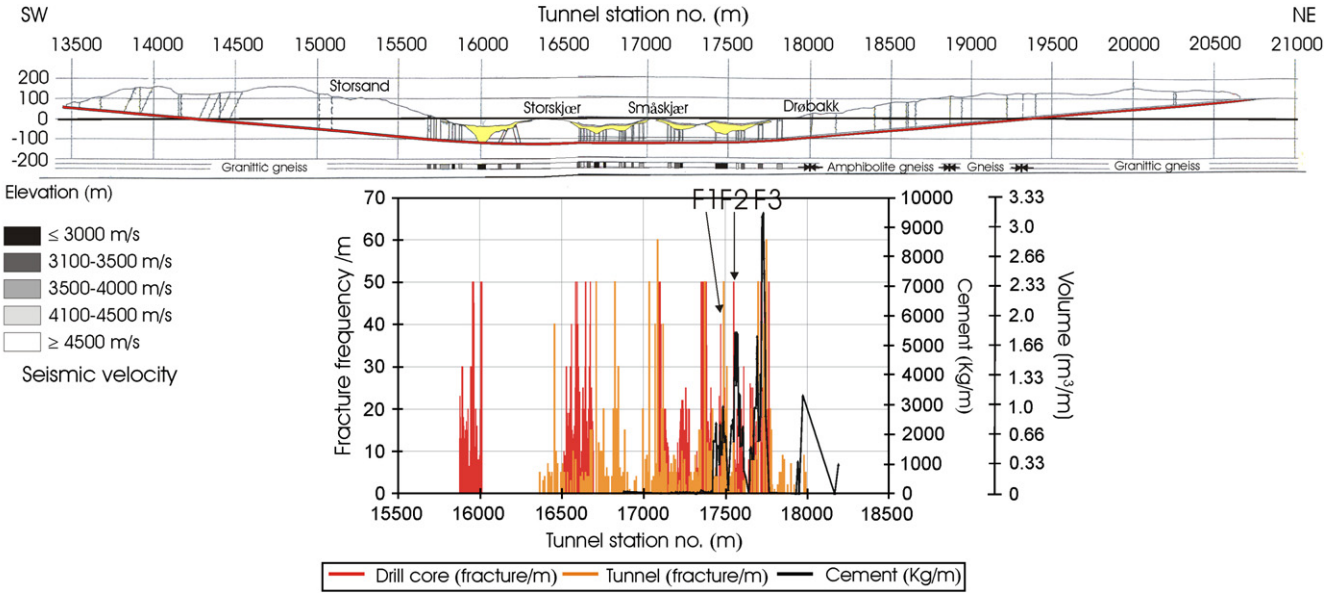

Fig. 5. Cross-section of the Oslofjord tunnel, also showing a plot of fracture frequency (tunnel mapping and drill core logs) and cement injection volumes. Peaks fit with faults for all datasets. This comparison of fracture frequency logged in the tunnel and in drill cores show that the fracture distribution is overall higher in the drill cores.

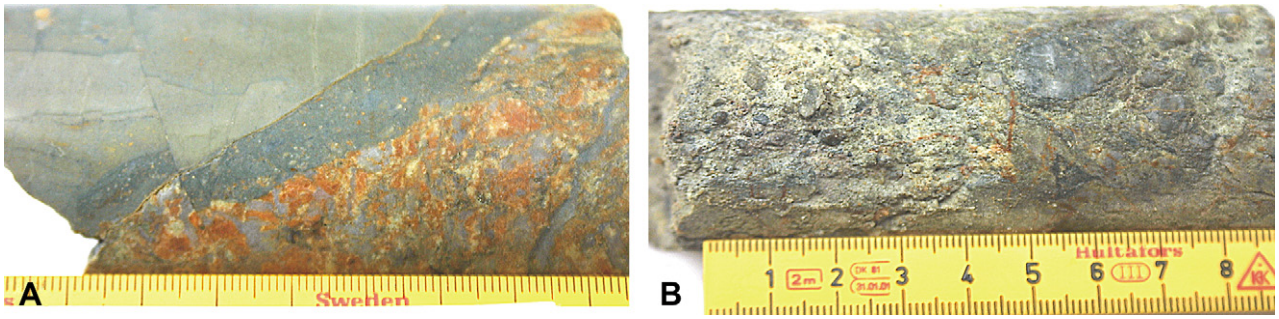

Fig. 6. Examples of fault rocks encountered in the Oslofjord tunnel. (A) Photograph of core showing a range from protocataclasite (right), cataclasite (center) to ultracataclasite (left). The cataclasites host fragments of protolith. (B) Photograph of protobreccia to the right that gradually transgress into a breccia to the left. The non-consolidated, porous breccias contain fragments of cataclasite in a fine grained matrix.

reflecting deformation spanning from ductile/plastic to brittle regimes (Swensson, 1990).

The OF in the Drøbaksundet strait consists of at least four strands, as can be demonstrated in the Oslofjord sub-sea tunnel (Fig. 5). Of these, the easternmost, major fault strand with assumed displacement of 2 km, dips to the west (synthetic), whereas the two central strands are nearly vertical. The westernmost fault zone host cores that dip both west and east. In more detail, the tunnel excavation revealed 25 small and large fault and/or fracture zones, most with decimetre to metre thick zones of cohesive and/or non-cohesive fault rocks in the fault core (Fig. 5; Statens vegvesen, 2001). Otherwise, the bedrock was regarded as of relatively good quality (Statens vegvesen, 2001). During construction three main faults were of concern. The western fault around station no. 16000 (Fig. 5) was deeply eroded and filled with an approximately 100 m wide section of non-consolidated sedimentary rocks. This zone was pre-grouted, frozen in advance and excavated very carefully, and then fully armoured (Statens vegvesen, 2001). At about station no. 16750, a 17–20 m wide fault core filled with gouge (clay rich) and highly fractured rock in the damage zone caused stability problems. Further east, at about station no. 17600, excavation of the main fault revealed extensively deformed rocks. The latter can be divided into a western part (station no. 17320–17350) and eastern part (station no. 17690–17715). The former has a fault core of mainly gouge (clay) hosting highly fractured rock, and caused extensive water inflow (Figs. 5 and 7). In the eastern part, the fault zone is dominated by densely fractured rock, which required extensive cement injection (Statens vegvesen, 2001), as reflected in Fig. 5. In this case, significant injection volumes match the greatest water leakage in the tunnel, of 30 l/min/100 m. For comparison, after finishing the tunnel, total leakage along the entire tunnel was 8 l/min/100 m (Statens vegvesen, 2001). The core and highly fractured parts of the eastern, main fault was immediately fully armoured during construction (Statens vegvesen, 2001).

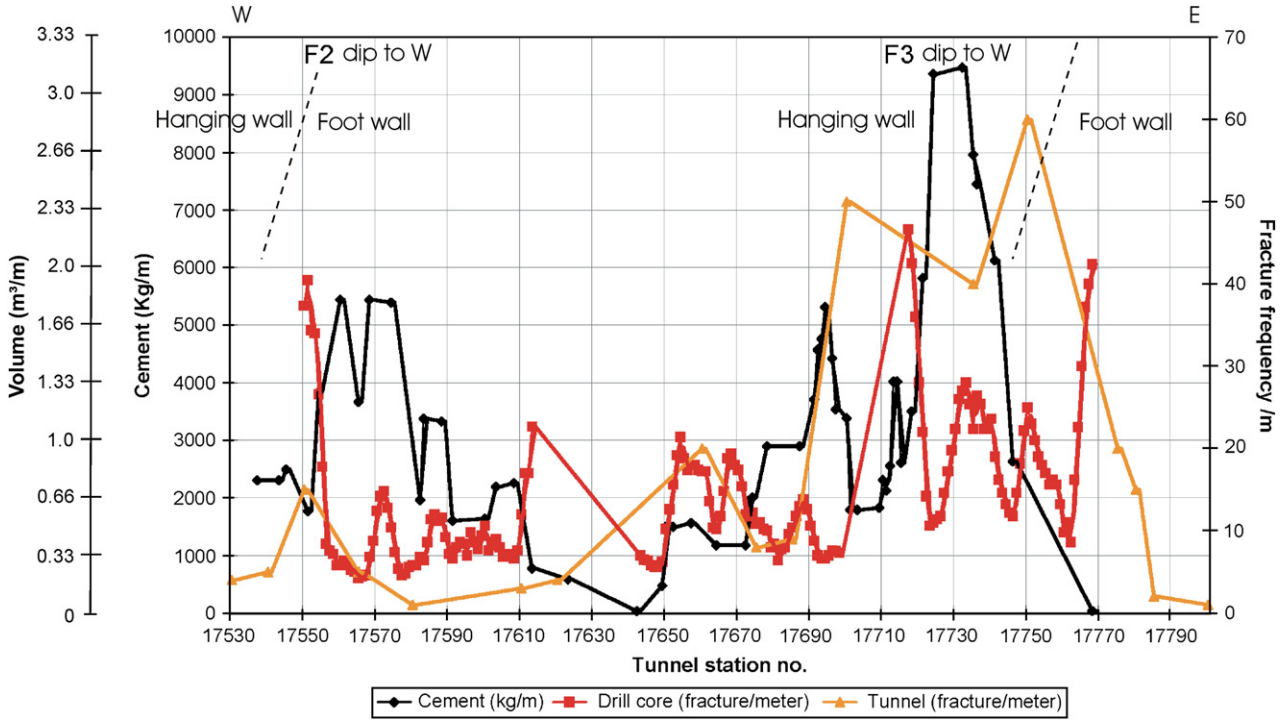

Fig. 7. Fracture distribution from logged drill cores and tunnel scan lines correlated with volume of injected cement for a section (station no. 17530–17800) of the Oslofjord tunnel. This tunnel section had the largest groundwater leakage and required the most pre-grouting. The peak of cement injected lies on both sides of the less permeable fault core, in the inner damage zone of the fault zone, as demonstrated at about st. no. 17550– 17590 and st. no. 17710– 17760. Note how the drops in cement volumes correlate with the position of fault cores.

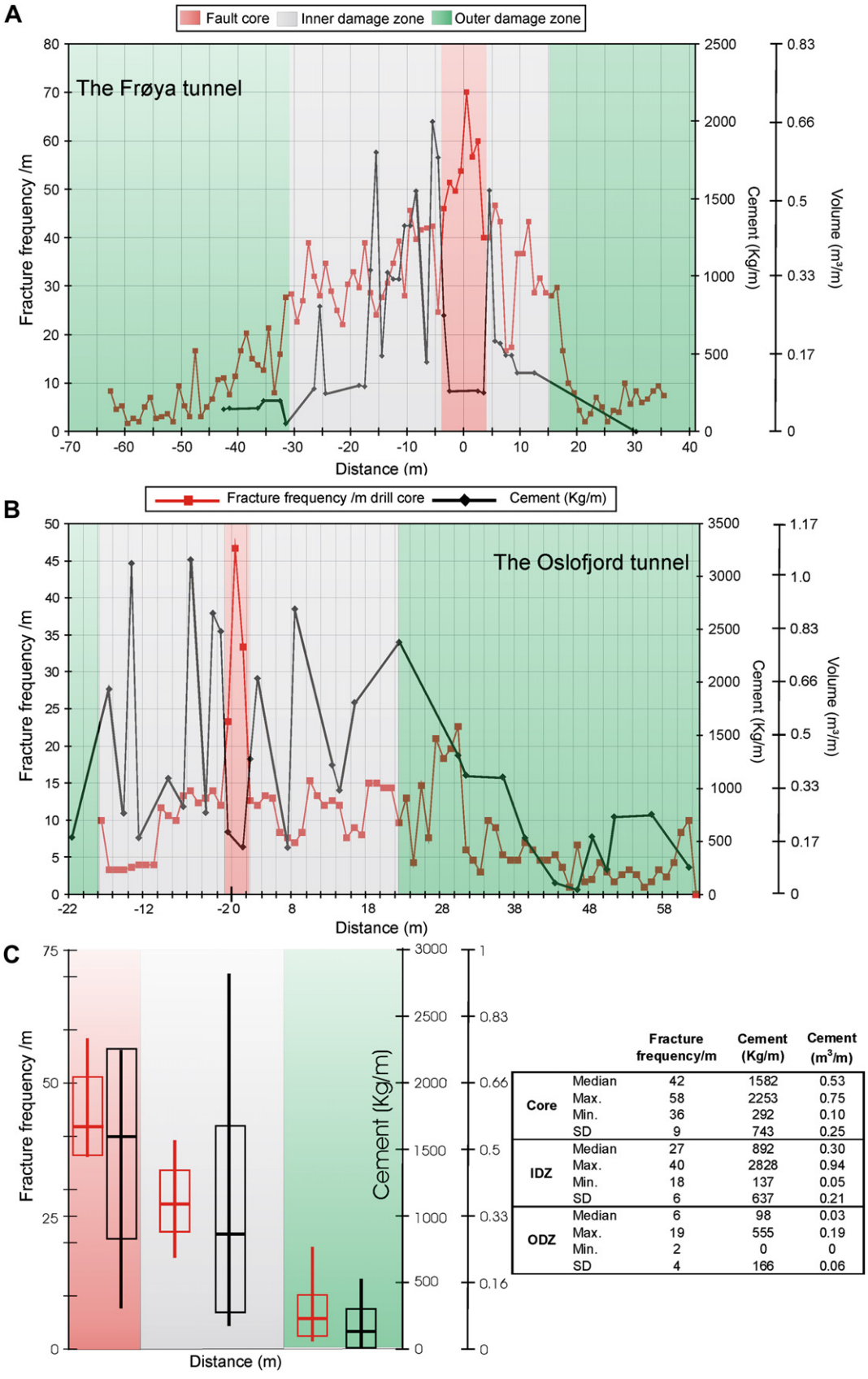

		Fracture frequency/m	Cement (Kg/m)	Cement (m^3/m)
Core	Median	42	1582	0.53
	Max.	58	2253	0.75
	Min.	36	292	0.10
	SD	9	743	0.25
IDZ	Median	27	892	0.30
	Max.	40	2828	0.94
	Min.	18	137	0.05
	SD	6	637	0.21
ODZ	Median	6	98	0.03
	Max.	19	555	0.19
	Min.	2	0	0
	SD	4	166	0.06

The drill cores show three events of deformation, as documented in fault cores. The oldest event is represented by (i) semi-ductile to ductile shear zone with augen clasts in a mylonitic matrix. This fabric is reworked in (ii) cataclasites that occur in sparse bands with millimetre to centimetre width or in the core of larger faults, then with metre width (Fig. 6A). The final activity on the fault is seen as (iii) non-cohesive breccia and gouge, hosting fragments of both the cataclasites and mylonites (Fig. 6B). This late, superimposed deformation rejuvenates the porosity of the fault cores, since the non-cohesive fault rocks are porous, contrary to the mylonites and cataclasites. However, non-cohesive fault rocks are less abundant than the cohesive ones.

For most faults mapped in the tunnel, the common width of fault zones is 60–100 m, frequently showing an increase in fracture frequency towards the core of the fault (Fig. 5). The fracture frequency in the drill cores outside fault zones reveals a background fracture level of 1–5 f/m. Within fault zones, peaks with fracture frequency between 30 and 50 f/m locate the cores of faults. Such peaks have maximum widths of up to 10 m, and are made up of breccias and gouge in the drill cores. The damage zones divide into wider parts with a fracture frequency in the range of 5–20 f/m, and narrower parts with values in the range or 20–30 f/m (Fig. 7). The latter is commonly found near or along the margin of fault cores, making up inner damage zones.

Injection volumes in the studied section of the Oslofjord tunnel (between station no. 15675 and 18190) is in general low, below 100 kg/m (0.03 m^3 per metre tunnel), with a total volume of 1811 tons (603.66 m^3) cement injected in the 2.4 km long tunnel section under the fjord. Peaks in injection volumes match the location of fault zones (Fig. 5). The best example is represented by the main fault occurring between station no. 17690 and 17750, which required extensive cement injection, a total of 682 tons (227.33 m^3). This fault zone, and especially the part with significant water leakage, required about 40% of the total cement volume over a distance of 60 m (Fig. 7). When correlating the fracture distribution (note preset values for fault rock) to the cement injection for this fault zone, as shown in Fig. 7, the peak of injected cement volume drops in the fault cores (stations 17705 and 17770). Contrary, in the marginal parts around the cores, in the inner damage zones, significant volumes are injected.

6. Discussion

6.1. Fault zone characteristics

Although the geological history of the two study sites is different, there are similarities in the fault characteristics. All faults intersected by the tunnels show a fault zone of 50–100 m width, where the fracture frequency commonly increases towards the core of the fault. Further, a polyphase history characterise the studied faults, with fault products including impermeable mylonites and cataclasites, which are reworked in porous breccias and gouge. In the Oslofjord tunnel the fault cores are in general narrow, seldom more than 10 m wide, and characterized by cataclasites superimposed by non-cohesive fault rocks. Contrary, the main faults intersected by the Frøya tunnel show up to 30 m wide fault cores mainly consisting of non-cohesive fault rock (Figs. 3 versus 6). Further, the fracture frequency, especially in the damage zone, is higher in the Frøya tunnel than in the Oslofjord tunnel. Apart from these minor differences, the structural characteristics of all described faults follow that commonly presented in the literature (Sibson, 1986, 2000; Chester et al., 1993; Caine et al., 1996; Braathen et al., 2004, Collettini and Holdsworth, 2004).

The detailed descriptions of major faults transected by the tunnels reveal common fault rocks surrounding intensively fractured rock lenses in the core. Encountered fracture frequencies in these lenses are commonly around 50 f/m, but can locally reach 100 f/m before the rock disintegrate to breccia. In the surrounding damage zones, networks of fracture sets can be divided into two parts, one that is made up of fairly high frequencies (20–30 f/m) and another with lower frequencies ($<$ 20 f/m). The part with higher frequencies are mostly found as a narrow zone marginal to the core (inner damage zone), whereas the lower frequency part covers the stretch outwards to background fracture level (outer damage zone). Outcrop studies by Braathen et al. (1998) suggest that the high frequency sub-zone has longer, fault sub-parallel structures, whereas the latter sub-zone is characterized by more diverse fracture orientations and lengths. This difference has significant implications for the permeability field in the damage zone, since longer fractures will conduct more water than short fractures, due to higher connectivity (Odling, 1997). Hence, due to higher frequencies and longer fractures in the inner damage zone, this sub-zone of faults should show higher injection values compared to the outer damage zone.

6.2. Fault zone permeability

The overall differences in structural characteristics between faults in the Frøya and Oslofjord tunnels may affect porosity and permeability properties. If this is so, the Oslofjord faults with narrow cores and less abundant porous fault rock and also lower fracture frequency in damage zones, should in general see less injection of cement. Contrary, faults of the Frøya tunnel have wide cores of both porous breccia and impermeable gouge, and also higher fracture frequency in the damage zones. When comparing results of the two tunnels, as presented in Fig. 8, the datasets from the damage zones contradicts the assumption presented above. There is slightly higher cement injection values for damage zones of the Oslofjord tunnel, with 0.7–1.1 m^3 per metre tunnel compared to 0.5–0.7 m^3/m for Frøya. Fault core injection volumes are also fairly similar, in the range of 0.1–0.15 m^3 per metre tunnel. In other words, the resolution of the datasets (see below) is not sufficient for detailed comparison of the permeability characteristics of individual faults.

Despite this negative result, common experience by engineers analysing tunnel constructions (Blindheim and Øvstedal, 2002) is that the core of the fault zone does not cause large inflow, since it usually contains impermeable fault rocks such as gouge (clay rich).

Fig. 8. (A) Correlation between fracture frequency in drill cores and injected cement per metre tunnel, presented as running average of 2 points for presentation purposes. The data are from three faults in the Frøya tunnel (see Fig. 2 for fault locations). The sub-zones of the fault are based on the distribution of fractures and fault rocks. In general, the trend show that the mass of injected cement is largest in the inner damage zone, with a distinct drop in the fault core and a relatively stable, low level in the outer damage zone. The cement volumes in the fault core are in general similar to those of the outer damage zone. (B) Correlation between fracture frequency in drill cores and injected cement per metre tunnel for three faults in the Oslofjord tunnel, presented as running average of 2 points for presentation purposes. See Fig. 5 for location of faults. The fault zoning is based on the distribution of fractures and fault rocks, as described in the text. For this dataset as well, the trend is that the volume of injected cement is largest in the inner damage zone, with a distinct drop in the fault core and a relatively stable, low level in the outer damage zone. The width of the fault core corresponds to the width of the drop in cement volume. (C) Plot presenting statistical values for fracture frequency (fractures/m) and cement injection data (kg/m and m^3/m) for the fault core, and the inner and outer damage zones, based on the six faults described in A and B. Values presented are average frequency and injection volume, standard deviation outlining the box, and maximum and minimum values delimiting the vertical line and median value the horizontal line, see also coherent table. Fracture frequencies for the fault core are preset values, see text. The high cement volumes in the fault core are probably due to the lack of detail in the cement dataset, where narrow fault cores (5–10 m wide) are overshadowed by interval of cement injection, see text for further explanation.

Large inflow is commonly found in the damage zone of the fault, where open fractures conduct water, similar to the model of Evans et al. (1997). For construction planning, locating such zones is of special interest since the combination of poor stability and water inflow presents a high risk of collapse (Blindheim and Øvstedal, 2002).

A fruitful examination addresses general fault zonation against injection patterns, as shown in Figs. 8 and 9, and presented in Table 1. The different zones of faults in both tunnels seem compatible in that there is a general pattern showing that the inner damage zone requires the highest volume of injected cement, while the less permeable fault core and outer damage zone show a distinct drop in the cement volume injected. To further test this pattern, three faults intersected by the Frøya tunnel were chosen for a detailed study (Table 1, Fig. 8A). In this dataset, the outer damage zone has average cement injection volumes of 150 kg/m (0.05 m^3/m), and fracture frequency in the range of 5–15 f/m. For the inner damage zone, the cement volumes are in the range of 1000–1500 kg/m (0.33–0.5 m^3/m), with a width of the sub-zone from 12 to 30 m that has a fracture frequency in the range of 25–45 f/m. The average thickness of the fault core is about 8 m, with a peak fracture frequency in rock lenses hosted by fault rocks of 60–70 f/m, and an average cement volume of 260 kg/m (0.08 m^3/m). This gives an injection average ratio of inner damage zone and fault core of approximately 2.3/1, core and outer damage zone ratio of 0.8/1, and inner and outer damage zone ratio of 3.1/1 (Table 1).

Similar patterns of injection can be found for the three studied faults in the Oslofjord tunnel (Fig. 8B), with an injection average ratio of inner damage zone and fault core of approximately 1.8/1, core and outer damage zone ratio of 1.1/1, and inner and outer damage zone ration of 1.7/1 (Table 1). However, there are exceptions; fault 3 in the Oslofjord tunnel gives the largest water leakage in the tunnel (see also Fig. 7). This fault has a wide damage zone of densely fractured rock and a narrow (0.5–1 m) fault core. With such a narrow core, the expected low ratio in cement volume of the fault core may be overshadowed by the damage zone, and therefore not show up, as discussed below. Fault 2 in the Frøya tunnel is another zone that caused significant water leakage. Again, a narrow core may explain why the volume ratios differ greatly from the other results (Table 1).

6.3. Resolution in datasets and permeability considerations

A major challenge in in situ analysis of faults is the different resolutions of available datasets. That is, drill cores reveal results on mm to metre scale, whereas tunnel data commonly covers intervals on metre-scale, in our case with intervals of 5–15 m. The engineering data such as the injected cement is related to excavation campaigns, commonly of 5 m length, setting off a new swarm of drill-holes ahead of the tunnel face. These drill holes are 23–30 m long (Lillevik et al., 1998; Lien et al., 2000; Statens vegvesen, 2001; Blindheim and Skeide, 2002; Blindheim and Øvstedal, 2002; Palmstrøm et al., 2003). The permeability fields along these holes are unknown but assumed to be more permeable near the tip, in the previously un-injected 5 m section at the base of the hole. Therefore, standard engineering results on pre-grouting can at best be considered viable on 5 m scale, and can only be regarded exact on 20–30 m scale. This lends support to the discussion above, in that structural zoning of faults below a minimum 5-m threshold may not be revealed in injection data, as suggest for some faults.

Despite such limitations in injection data, one can crudely calculate effective porosity of the rocks. The drill hole swarm generally covers an area of around 200–300 m^2, which can be converted to 200–300 m^3 for one metre of tunnel. With the average injection

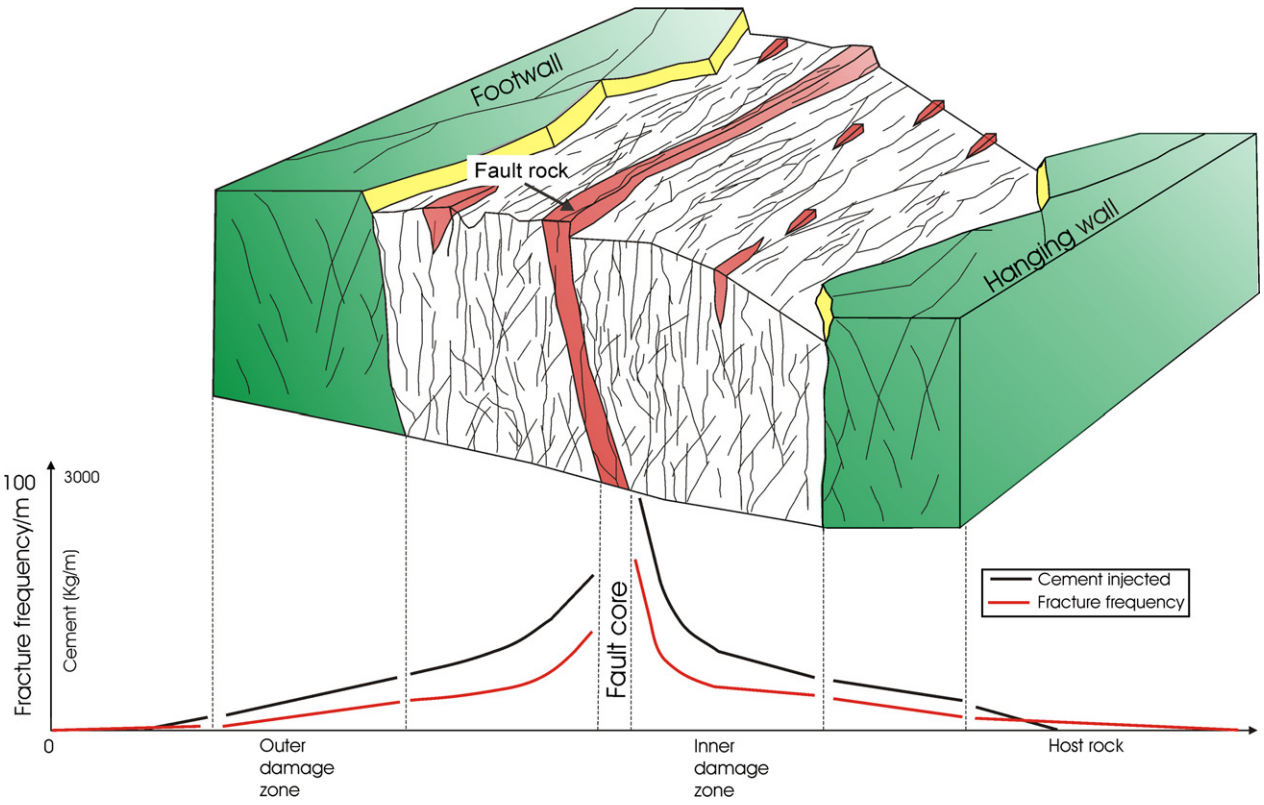

Fig. 9. Conceptual model of extensional faults in metamorphic and crystalline rocks, divided into sub-zones (modified after Braathen and Gabrielsen, 2000). The curves describe anticipated fracture frequency of the damage zone and volumes of injected cement (pre-grouting) into the fault zone. Note that the model predicts increase in fracture frequency from a linear trend in the outer damage zone to a possible exponential trend in the inner damage zone. Some cases may also see a small asymmetry, with more intense deformation and thereby increased injection in the hanging-wall of the fault. See text for discussion.

Table 1
Amount of injected cement and their characteristics in the different sub zones, the fault core (C), the inner damage zone (ID) and the outer damage zone (OD) of totally six faults in the two sub-sea tunnels

Faults	Station no.	Fault core (C)				Inner damage zone (ID)				Outer damage zone (OD)				Ratio ID/C	Ratio OD/C	Ratio ID/OD
		Cement (kg/m)	Volume (m^3/m)	FF (preset max/m)	Width (m)	Cement (kg/m)	Volume (m^3/m)	FF (max/m)	Width (max, m)	Cement (kg/m)	Volume (m^3/m)	FF (max/m)	Width (min, m)			
The Oslofjord tunnel																
OF fault 1	17470–17520	1351	0.45	40	3	(HW) 2946	0.98	25	26	(HW) 1937	0.65	15	16	2.2	1.4	1.5
OF fault 2	17550–17580	691	0.23	50	4	(FW) 1247	0.42	20	46	(FW) 642	0.21	12	10	1.8	0.9	1.9
OF fault 3	17720–17750	6787	2.26	50	2	(HW) 9479	3.16	30	18	(HW) 5820	1.94	18	8	1.4	0.9	1.6
The Frøya tunnel		*Average*	0.98				1.52				0.93			1.8	1.1	1.7
F fault 1	3970–4010	857	0.29	70	44	(FW) 1523	0.51	30	30	(FW) 667	0.22	15	5	1.8	0.8	2.3
F fault 2	4090–4160	1474	0.49	70	27	(FW) 4651	1.55	22	12	(FW) 895	0.30	12	20	3.2	0.6	5.2
F fault 3	5390–5420	732	0.24	70	5	(FW) 1464	0.49	27	20	(FW) 776	0.26	12	5	2	1.1	1.9
	Average		0.34				0.85				0.26			2.3	0.8	3.1
	Total average		0.66				1.18				0.60			2	0.9	2.4

OF – Oslofjord faults; F – Frøya faults. Ratio of cement injected in the different zones of the fault, showing characteristics of the three faults selected from each tunnel and their coherent zones. HW – hanging-wall; FW – footwall; FF – fracture frequency.

volumes established herein (see below), effective porosities for cement is low, in the range of 0.50% for the inner damage zone, c. 0.25% for the core and outer damage zone, and below 0.01% for the protolith. We stress that this are guiding numbers rather than exact facts, since the calculations are hampered with significant uncertainty.

Porosity calculations and permeability assessments are in general challenged by the heterogenic nature of fracture aquifers, which will flavour interpretations of injection data in a swarm of drill holes ahead of a tunnel. For example, a single long and highly permeable fracture may conduit cement far out from the tunnel profile, and thereby trigger injection in a large volume of porous, fractured rocks. Without this fracture, the volume of available porous rock would be significantly smaller. Such long and highly permeable fractures are occasionally experienced in shallow tunnels, where they are documented by pre-grouting cement that burst out on the surface (Danielsen and Dahlin, 2006, 2007). However, even with these uncertainties, it is likely that large-scale in situ injection data is better representing fault porosity and permeability fields than the up-scaled result of laboratory measurements of selected structures within major fault zones (Morrow and Byerlee, 1988, 1992; Evans et al., 1997; Seront et al., 1998; Wibberley and Shimamoto, 2003), where the flow characteristics of faults are established through numerical models.

6.4. Permeability models of faults in metamorphic and crystalline rocks

As outlined, most detailed outcrop studies of fault zones show an increase in fracture frequency towards the fault core (Fig. 9), in some cases even supporting a difference in the fracture distribution between a wider hanging-wall and a narrower footwall (e.g., Caine et al., 1996; Braathen et al., 1998; Gudmundsson et al., 2001; Micarelli et al., 2003; Berg and Skar, 2005). Further, for example Berg and Skar (2005) suggest that there is a linear trend of structural frequency in the distal part of fault zones (in sandstone), in the outer damage zone, which evolves into an exponential trend in the inner damage zone. In our analysis, two of six faults have a damage zone side consistent with this view. Anyhow, the pattern of significantly increased injection volumes in the inner damage zone is well documented above, and can be explained by such an empiric model through fracture frequency alone. Alternatively, the explanation may be a general pattern of higher fracture frequencies and longer fractures in the inner damage zone, or a combination of the two models.

Despite the presented contrary examples presented above, the general results from this study agree well with results presented by for example Evans et al. (1997), which show that the damage zone has the highest permeability. However, the proposed fault zone contrast, with permeability 10–1000 times lower in the fault core and the protolith compared to the damage zone, seems very high compared to our results on in-site fault permeability. At the best, such contrasts may be valid in comparisons between the inner damage zone and an un-fractured protolith domain. Our combined study of quantitative fault zone descriptions, qualitative fracture and fault rock property assessments, and engineering pre-grouting data sustains the conclusion that there is much more cement injected into the inner damage zone than in the fault core and the outer damage zone (ratio $\sim$ 2:1, Table 1). Average injection volumes of cement per metre tunnel for the fault core is 0.66 m^3, for the inner damage zone is 1.18 m^3, and for the outer damage zone is 0.60 m^3 (Table 1). Therefore, there is about the same amount of cement injected into the core as the outer damage zone ($\sim$1:1, Table 1). Injected volumes in the background domain of the protolith are insignificant, in accordance with the conclusions drawn by Morrow and Byerlee (1988, 1992), Evans et al. (1997), and Seront et al. (1998).

7. Conclusions

This study of extensional fault zones in granites and gneisses combine datasets from two tunnels, including scan-lines, drill cores, and pre-grouting cement volumes. The following conclusions can be drawn from the analysis:

1) Fault zones show an increase in fracture frequency from the background fracture level in protolith towards the fault core.
2) Fault zones can be divided into a core, inner damage zone, and outer damage zone with basis in structural characteristics.
3) There is a substantial increase in injected cement volumes in fault zones compared to areas with background fracturing.
4) Fault cores show a clear reduction in injected cement compared to the inner damage zone, likely caused by abundant impermeable fault rocks in the core.
5) High injection values in the inner damage zone likely relates to a high frequency of long, fault-parallel fractures with good connectivity, whereas lower injection volumes in the outer damage zone is controlled by lower fracture frequencies and more variable fracture orientations and lengths.
6) Average injection volumes of cement per metre tunnel for the fault core is 0.66 m^3 (SD = 0.79), for the inner damage zone is 1.18 m^3 (SD = 1.06), and for the outer damage zone is 0.60 m^3 (SD = 0.68).

7) Injection volume of cement has a relative relationship of 1:2:1 between fault core, inner damage zone and outer damage zone.

Acknowledgement

Thanks go to the engineering geologists Heidi Berge (Oslofjord tunnel) and Stig Lillevik (Frøya tunnel) at Statens vegvesen for access to tunnel data, and Kristin Holmøy, NTNU, for helpful comments on tunnel data. Thanks to Steve Rogers and an anonymous person, whose review comments contributed to improve this paper.

References

Askvik, H., Rokoengen, K., 1985. Bedrock map KRISTIANSUND. Geological Survey of Norway, scale 1 250 000.
Berg, S.S., Skar, T., 2005. Controls on damage zone asymmetry of a normal fault zone: outcrop analysis of a segment of the Moab fault SE Utah. Journal of Structural Geology 27, 1803–1822.
Blindheim, O.T., Øvstedal, E., 2002. Design principles and construction methods for water control in subsea road tunnels in rock. Norwegian Tunneling Society 12, 43–49.
Blindheim, O.T., Skeide, S., 2002. Determination and co-operation is crucial for rock mass grouting in order to satisfy strict environmental requirements. Norwegian Tunneling Society 12, 89–95.
Bøe, R., Mørk, M.B.E., Roberts, D., Vigran, J.O., 2005. Possible Mesozoic Sediments in Fault and Brecciation Zones in Frøyfjorden, Mid-Norway. NGU Bulletin 443. Geological Survey of Norway, 29–35.
Braathen, A., 1996. Bruddsoner på Frøya og Nord-Hitra. NGU report 96.023. Geological Survey of Norway, 1–15 (in Norwegian).
Braathen, A., Gabrielsen, R., 2000. Bruddsoner i fjell – oppbygning og definisjoner. Norges geologiske undersøkelse. Gråsteinen 7, 1–20 (in Norwegian).
Braathen, A., Gabrielsen, R.H., Henriksen, H., Lothe, A., Midtbø, E., Midtgård, A.K., Berg, S., Lyslo, K., Skurtveit, E., 1998. Lineament architecture and distribution in metamorphic and sedimentary rocks, with application to Norway. NGU Report 98.043, Geological Survey of Norway, 1–78.
Braathen, A., Osmundsen, P.T., Gabrielsen, R.H., 2004. Dynamic development of fault rocks in a crustal-scale detachment: an example from western Norway. Tectonics 23 (TC 4010), 1–21.
Caine, J.S., Evans, J.P., Forster, C.B., 1996. Fault zone architecture and permeability structure. Geology 24 (11), 1025–1028.
Chester, F.M., Chester, J.S., 1998. Ultracataclasite structure and friction processes of the Punchbowl fault, San Andreas system, California. Tectonophysics 295, 199–221.
Chester, F.M., Evans, J.P., Biegel, R.L., 1993. Internal structure and weakeningmechanisms of the San Andreas Fault. Journal of Geophysical Research-Solid Earth 98 (B1), 771–786.
Collettini, C., Holdsworth, R.E., 2004. Fault zone weakening and character of slip along low-angle normal faults: insights from the Zuccale fault, Elba, Italy. Journal of the Geological Society, London 161, 1039–1051.
Danielsen, B.E., Dahlin, T., 2006. Geophysical and Hydraulic Properties in Rock. Conference processing. 12th European Meeting of Environmental and Engineering Geophysics, 4–6 September 2004, Helsinki, Finland, 4 p.
Danielsen, B.E., Dahlin, T., 2007. Comparison of geoelectrical imaging and tunnel documentation. Submitted to Engineering Geology.
Eliassen, H.E., 2003. Sen-kaledonske og yngre (mesosoiske og kenosoiske) forkastninger på Frøya, Møre-Trøndelag kysten. MSc thesis unpublished, pp. 1–232 (in Norwegian).
Evans, J.P., Chester, F.M., 1995. Fluid-rock interaction in faults of the San-Andreas system – inferences from San-Gabriel fault rock geochemistry and microstructures. Journal of Geophysical Research-Solid Earth 100, 13007–13020.
Evans, J.P., Forster, C.B., Goddard, J.V., 1997. Permeability of fault-related rocks, and implications for hydraulic structure of fault zones. Journal of Structural Geology 19, 1393–1404.
Faulkner, D.R., Rutter, E.H., 2001. Can the maintenance of overpressured fluids in large strike-slip fault zones explain their apparent weakness? Geology 29 (6), 503–506.
Faulkner, D.R., Lewis, A.C., Rutter, E.H., 2003. On the internal structure and mechanics of large strike-slip fault zones: field observations of the Carboneras fault in southeastern Spain. Tectonophysics 367, 235–251.
Gabrielsen, R.H., Braathen, A., Dehls, J., Roberts, D., 2002. Tectonic lineaments of Norway. Norwegian Journal of Geology (NGT) 82, 153–174.
Gee, D.G., Guezou, J.C., Roberts, D., Wolff, F.C., 1985. The central-southern part of the Scandinavian Caledonides. In: Gee, D.G., Sturt, B.A. (Eds.), The Caledonide Orogen-Scandinavia and Related Areas. Wiley, Chichester, pp. 109–134.
Grønlie, A., Nilsen, B., Roberts, D., 1991. Brittle deformation history of fault rocks on the Fosen Peninsula, Trøndelag, Central Norway. NGU Bulletin 421, 39–57.
Gudmundsson, A., Berg, S.S., Lyslo, K.B., Skurtveit, E., 2001. Fracture networks and fluid transport in active fault zones. Journal of Structural Geology 23, 343–353.
Heeremans, M., Larsen, B.T., Stel, H., 1996. Paleostress reconstruction from kinematic indicators in the Oslo Graben, southern Norway: new constraints on the mode of rifting. Tectonophysics 266, 55–79.
Hoek, E., 2000. Rock Engineering – Course Notes by Evert Hoek. http://www.rocscience.com/hoek/PracticalRockEngineering.asp.
Hoek, E., Bray, J.W., 1981. Rock Slope Engineering, third ed. Institution of Mining and Metallurgy. 358.
Lien, J.E., Lillevik, S., Mehlum, A., Soknes, S., 2000. Frøyatunnelen – fra geologisk kartlegging til ferdig tunnel. In: Fjellspregningsteknikk, Bergmekanikk/Geoteknikk, pp. 6.1-6.46 (Conference proceeding, in Norwegian).
Lillevik, S., Holmøy, K.H., Lien, J.E., 1998. Frøyatunnelen – Passering av problemsoner – Erfaringer fra kartlegging og faktiske forhold. In: Fjellspregningsteknikk, Bergmekanikk/Geoteknikk, pp. 32.1-32.22 (Conference proceeding, in Norwegian).
Lutro, O., Nordgulen, Ø., 2004. Bedrock map of the Oslo area, Norway, Geological Survey of Norway. scale 1 250,000.
Manzocchi, T., Heath, A.E., Palananthakumar, B., Childs, C., Walsh, J.J., 2008. Faults in conventional flow simulation models: a consideration of representational assumptions and geological uncertainties. Petroleum Geoscience 14 (1), 91–110 (20).
Micarelli, L., Moretti, I., Daniel, J.M., 2003. Structural properties of rift-related normal faults: the case study of the Gulf of Corinth, Greece. Journal of Geodynamics 36, 275–303.
Morrow, C., Byerlee, J., 1988. Permeability of rock samples from Cajon Pass, California. Geophysical Research Letter 15 (9), 1033–1036.
Morrow, C., Byerlee, J., 1992. Permeability of core samples from Cajon Pass scientific drill hole: results from 2100 to 3500 m depth. Journal of Geophysical Research 97 (B4), 5145–5151.
Morrow, C.A., Lockner, D.A., 1997. Permeability and porosity of the Illinois UPH 3 drillhole granite and a comparison with other deep drillhole rocks. Journal of Geophysical Research 102 (B2), 3067–3075.
Nilsen, B., Palmstrøm, A., 2000. Engineering Geology and Rock Engineering. Handbook No. 2. Norwegian Group for Rock Mechanics (NBG), pp. 249.
Nordgulen, Ø, Solli, A., Sundvoll, B., 1995. Caledonian granitoids in the Frøya area, central Norway. NGU Bulletin 427, 48–51.
Norton, D., Knapp, R., 1977. Transport phenomena in hydrothermal systems; the nature of porosity. American Journal of Science 277 (8), 913–936.
Odling, N.E., 1997. Scaling and connectivity of joint systems in sandstone from western Norway. Journal of Structural Geology 19 (10), 1257–1271.
Osmundsen, P.T., Eide, E., Haabesland, N.E., Roberts, D., Andersen, T.B., Kendrick, M., Bingen, B., Braathen, A., Redfield, T.F., 2006. Kinematics of the Høybakken detachment zone and the Møre-Trøndelag fault complex, Central Norway. Journal of the Geological Society, London 163. 303-318.
Palmstrøm, A., Nilsen, B., Pedersen, K.B., Grundt, L., 2003. Miljø- og samfunnstjenlige tunneler – Riktig omfang av undersøkelser for berganlegg. Publ. No. 101, pp. 1–52 (in Norwegian).
Redfield, T.F., Braathen, A., Gabrielsen, R.H., Osmundsen, P.T., Torsvik, T.H., Andriessen, P.A.M., 2005. Late Mesozoic to Early Cenozoic components of vertical separation across the Møre-Trøndelag Fault Complex, Norway. Tectonophysics 395, 233–249.
Sættem, J., Mørk, M.B.E., 1996. SINTEF report 96.018. Frøytunnelen: Studie basert på vertikalboringer og regional lineament-informasjon, 1–35 (in Norwegian).
Seront, B., Wong, T.F., Caine, J.S., Forster, C.B., Bruhn, R.L., 1998. Laboratory characterization of hydromechanical properties of a seismogenic normal fault system. Journal of Structural Geology 20 (7), 865–881.
Sibson, R.H., 1986. Brecciation processes in fault zones: inferences form earthquake rupturing. Pure and Applied Geophysics 124, 159–175.
Sibson, R.H., 2000. Fluid involvement in normal faulting. Geodynamics 29, 469–499.
Statens vegvesen, September 2001. Sluttrapport. Oslofjordforbindelsen, 1–65 (in Norwegian).
Stewart, M., Strachan, R.A., Holdsworth, R.E., 1999. Structure and earlykinematic history of the Great Glen fault zone. Scotland. Tectonics 18 (2), 326–342.
Swensson, E., 1990. Cataclastic rock along the Nesodden Fault, Oslo Region, Norway: a reactivated Precambrian shear zone. Tectonophysics 178, 51–65.
Walsh, J.J., Bailey, W.R., Childs, C., Nicol, A., Bonson, C.G., 2003a. Formation of segmented normal faults: a 3-D perspective. Journal of Structural Geology 25 (8), 1251–1262.
Walsh, J.J., Childs, C., Imber, J., Manzocchi, T., Watterson, J., Nell, P.A.R., 2003b. Strain localisation and population changes during fault system growth within the Inner Moray Firth, Northern North Sea. Journal of Structural Geology 25 (2), 307–315.
Wibberley, C.A.J., Shimamoto, T., 2003. Internal structure and permeability of major strike-slip fault zones: the Median Tectonic Line in Mie Perfecture, Southwest Japan. Journal of Structural Geology 25, 59–79.